Assessment of mean world ocean meridional heat transport characteristics by a high-resolution model

K. V. Ushakov[1,2] and R. A. Ibrayev[1,2]

Received 7 October 2017; accepted 8 February 2018; published 28 February 2018.

Eddy-induced meridional heat transport (EMHT) distribution in the world ocean is calculated by means of the eddy-resolving model INMIO, with atmospheric and radiative forcing defined by the CORE-II protocol data in 1978–1982. The EMHT is defined as the deviation of the total MHT value from the one calculated on the basis of 3-month running means of temperature and velocity. Local and zonally-integrated distributions of the EMHT in the global ocean and its basins are considered. We show that in some locations the eddy component makes a significant contribution to the total MHT, particularly in the Southern Ocean, near the equator, in western boundary currents, and in the regions of current confluences. Several qualitative differences are found between our results and other model-based and observation-based assessments. The eddy heat transport is shown to have sometimes a positive component along the horizontal temperature gradient direction, which makes it ill-founded to parameterize the EMHT by the common heat diffusion law with a positive diffusion coefficient. *KEYWORDS:* World ocean; ocean general circulation model; high-resolution model; mesoscale eddies; eddy meridional heat transport.

Citation: Ushakov, K. V. and R. A. Ibrayev (2018), Assessment of mean world ocean meridional heat transport characteristics by a high-resolution model, *Russ. J. Earth. Sci., 18,* ES1004, doi:10.2205/2018ES000616.

1. Introduction

The world ocean plays an important role in the formation of the Earth climate due to its ability to transport heat from the tropical to polar latitudes. The average oceanic meridional heat transport (MHT) is of the same order of magnitude as the atmospheric one, and many studies highlight the importance of their coherence for maintaining a stable state of the climate system, e.g., [*Diansky and Volodin,* 2002; *Diansky et al.,* 2002; *Griffies et al.,* 2009; *Volodin et al.,* 2018] and references therein. Nowadays, the MHT mean distributions in the world ocean and its large basins are particularly studied from ships, buoys and satellite data with the help of inverse models and surface heat fluxes analysis [*Ganachaud and Wunsch,* 2003; *Hall and Bryden,* 1982; *Macdonald and Wunsch,* 1996; *Polonsky and Krasheninnikova,* 2015].

However, its spatiotemporal variability is poorly available to contact observations due to their low resolution, while satellite data do not give information about the distribution in the ocean interior. Another source of errors is the intra-annual nonuniformity of data due to the difficulties of contact observations in the cold season. The complexity of field studies makes mesoscale eddies one of the least

[1]Shirshov Institute of Oceanology, Russian Academy of Sciences, Moscow, Russia
[2]Institute of Numerical Mathematics, Russian Academy of Sciences, Moscow, Russia

http://rjes.wdcb.ru/doi/2018ES000616-res.html

observed and data-provided objects in the ocean. Therefore, attempts to directly restore the EMHT on the basis of contact measurements face large errors [*Flierl and McWilliams,* 1977]. Combination of satellite altimetry data and ARGO T, S-profiles allows us to obtain the eddy heat and fresh water transport distributions with spatial resolution of the order of several degrees [*Dong et al.,* 2014].

Meanwhile, mesoscale eddies make a substantial contribution to the heat and fresh water transport, including climatic timescales, e.g., [*Roemmich and Gilson,* 2001]. Satellite altimetry data show that eddies are widespread in the ocean, but their contribution to transport processes is important only in particular places, primarily associated with strong currents and confluences, such as the regions of western boundary currents, tropics, and the Antarctic Circumpolar Current (ACC). It is known that in such conditions the eddy heat transport is often directed opposite to the transport of the mean flow and may have a comparable magnitude [*Bryan,* 1996]. The eddies also provide a natural mechanism of heat transport across the mean flow streamlines. They play an important role in locations of vertical water flow, where they usually offset the mean heat transport directed into the ocean depths [*Morrison et al.,* 2013]. The authors of the study [*Dong et al.,* 2014] point to the water capture inside an eddy as the main mechanism of eddy meridional heat and salt transport. They also note that eddy contribution to the zonal transport is much smaller because of the mutual compensation of cyclone and anticyclone effects.

At present, numerical modeling remains the only instrument capable of reproducing the global three-dimensional structure of ocean mesoscale eddies and its impact on the ocean heat balance. Modern eddy-resolving models are able to solve ocean circulation equations with a global spatial resolution of 0.1° and higher, which is considered to be generally sufficient to simulate the mesoscale eddy dynamics [*Maltrud and McClean,* 2005; *Smith et al.,* 2000].

Usually the following formula is used to calculate MHT in the general circulation models:

$$Q = \iint F_V dzdx + \iint F_S dzdx \qquad (1)$$

where $F_V = \rho C_P \theta V$ is the explicitly resolved advective heat flux, V is the meridional component of the current velocity, θ is the potential temperature, ρ is the density, and C_P is the heat capacity of the ocean water. The F_S term stands for heat transport by subgrid processes, primarily by unresolved eddies and turbulent mixing. The integrals are taken over depth and longitude within the basin considered. In case of absence (or, at least, smallness) of the total water transport through the basin zonal section the Q value does not depend on the choice of the temperature scale (K or °C) and may be considered as an objective quantitative characteristic. In ocean general circulation models, the subgrid meridional heat flux is usually parameterized by the heat diffusion formula

$$F_S = -A_H \rho C_P \frac{d\theta}{dy} \qquad (2)$$

where the diffusion coefficient A_H may depend on grid parameters or local solution. With such choice of A_H, it is necessary to make various assumptions on the characteristics of the medium, which are often simplifying and insufficiently substantiated. For a long time, this approach was justified, showing a stable behavior of the model MHT and its gradual transition from parameterized scales to explicitly resolved ones with the increase of model resolution from coarse to medium [*Beckmann et al.,* 1994; *Meijers et al.,* 2007]. However, at the present level of numerical modeling development, discrepancies between the model results of different resolutions become qualitatively significant and parameterizations ambiguity grows [*Griffies et al.,* 2015]. Fresh water transport parameterizations face even larger errors [*Dong et al.,* 2014]. Hence, the general tendency of detailed ocean circulation modeling studies is to make the contribution of diffusion terms as small as possible, and to maximally explicitly resolve the ocean turbulent energy spectrum outside boundary layers by means of high resolution and small viscosity and diffusivity coefficients.

Herewith, the explicitly resolved EMHT may be assessed as the difference between the total MHT and its part determined by the mean flow and mean temperature fields (first two terms in (3)):

$$Q_E = \iint \rho C_P \theta V dzdx - \iint \rho C_P \langle\theta\rangle\langle V\rangle dzdx - \iint A_H \rho C_P \frac{d\theta}{dy} dzdx \qquad (3)$$

The last term represents the parameterized part of the EMHT. Angle brackets define the mean value

over a characteristic time scale of mesoscale eddies, which is about 1–3 months [*Gill,* 1982; *Volkov et al.,* 2008]. It is worth noting that this approach takes into account not only the actual eddy effects but also all other short-time elements of the ocean circulation (transients), including the meandering of currents, tropical instability waves and fast variability of the Ekman layer. Their contribution to the MHT is determined by correlations of rapidly varying fields of temperature and velocity. Traditionally all these effects are referred to as eddy heat transport, and we will use this term in our work. Note that the fluctuating part of velocity by definition satisfies the condition of zero mean flow through any chosen zonal section; hence, in the case of averaging over a sufficiently long time period the Q_E value does not depend on the choice of the temperature scale.

By means of such technique [*Jayne and Marotzke,* 2002; *Volkov et al.,* 2008, 2010] studied the global distributions of the EMHT on the basis of model data with 0.25° resolution. The studies in [*Meijers et al.,* 2007; *Yim et al.,* 2010] consider particular basins of the world ocean with higher resolution, and the authors of [*Griffies et al.,* 2015] give some characteristics of the eddy heat transport as a part of their global eddy-resolving model solution.

The goal of this work is to study the global ocean EMHT distribution. It follows the path of eddy-resolving modeling researches and is based on the INMIO world ocean model. The model has been recently verified and calibrated in numerical experiments on simulating the climatic MHT distribution in the global and Atlantic oceans with $0.5° - 0.1°$ resolution [*Ibrayev et al.,* 2012; *Ushakov et al.,* 2015, 2016]. The main principles and schemes of the model are based on the work [*Ibrayev,* 2001]. The study in [*Volodin et al.,* 2018] performs a CORE-II protocol comparison [*Griffies et al.,* 2012] of INMIO with another Russian ocean general circulation model INMOM [*Gusev and Diansky,* 2014] which uses other methods and schemes, particularly, the vertical σ-axis. Further in Section 2, general descriptions of the model and of the numerical experiment formulation are given. Section 3 considers the model spin-up. Section 4 is dedicated to the analysis of the numerical experiment results. Section 5 contains general discussion and conclusions.

2. Ocean General Circulation Model and Numerical Experiment Formulation

The INMIO model is designed for research of the circulation in the world ocean and its basins in a wide range of spatial and temporal scales. The 3DPEM system of ocean dynamics equations with hydrostatic and Boussinesq approximations (e.g. [*Gill,* 1982; *Sarkisyan and Sündermann,* 2009]) is discretized by the finite-volume method [*Bryan,* 1969] on B-type horizontal grid [*Lebedev,* 1964a, 1964b; *Mesinger and Arakawa,* 1976] and vertical z-axis.

In this work, we use the tripolar horizontal grid [*Murray,* 1996] with 0.1° resolution in its spherical part. Vertical axis consists of 49 levels with steps gradually increasing from 6 m in the upper layer to 250 m in the deep ocean. The fast barotropic dynamics is modeled by solving a shallow water equations system with the parallel overlapping algorithm [*Kalmykov and Ibrayev,* 2013]. Sea ice state is described by the thermodynamic model [*Schrum and Backhaus,* 1999]. On the ocean-atmosphere interface the nonlinear kinematic free surface condition is posed (e.g. [*Griffies et al.,* 2006]) with heat, water and momentum fluxes calculated by the CORE bulk formulae [*Griffies et al.,* 2009]. The momentum transport term is approximated by the centered difference scheme, and the heat and salt advection is discretized by the flux-corrected transport scheme [*Zalesak,* 1979]. Vertical turbulent mixing is parameterized with viscosity and diffusion coefficients depending on the Richardson number via the Munk-Anderson scheme [*Munk and Anderson,* 1948] with convective adjustment subroutine called in the case of unstable vertical density profile. Except vertical turbulent mixing, all equation terms are integrated by explicit time-stepping schemes which made it possible to effectively parallelize the model code for distributed-memory supercomputers. The model run is governed by the Compact Modeling Framework, which provides parallel halo exchanges, interpolation of data between atmosphere and ocean – sea-ice grids, and asynchronous I/O operations with almost linear parallel scaling up to 32 thousand cores [*Kalmykov et al.,* 2014].

The numerical experiment was performed with the diffusion coefficient A_H equal to 100 m^2/s at the equator and scaling on the globe proportionally to the square root of the gridbox area. To ensure numerical stability of momentum transport equations solving, we used the biharmonic viscosity term with coefficient – 18×10^9 m^4/s at the equator scaled proportionally to the gridbox area using 3/2 power function. The background values of vertical viscosity and diffusivity are 10^{-4} and 10^{-5} m^2/s, while maximal values (obtained in locations of small Richardson numbers) equal to 10^{-2} and 10^{-3} m^2/s, respectively. The time steps are 4 min. for the main model cycle (baroclinic equations) and 5 sec for shallow water equations.

The major factors restricting the use of global eddy-resolving models are the costs of computational resources and storage. Therefore, general eddy-resolving experiment duration is currently of the order of several years or first decades, e.g., [*Marzocchi et al.,* 2015]. In this work, we performed calculations for five model years (1978–1982) under the conditions of the CORE-II protocol [*Griffies et al.,* 2012], which defines atmospheric parameters, radiative forcing, precipitation and continental runoff. Since the experiment duration is small, we did not apply relaxation of surface temperature or salinity to climatic data, which was used in long-term experiments of [*Griffies et al.,* 2009] to avoid model climate drift. The model integration starts from the T, S fields of WOA09 [*Antonov et al.,* 2010; *Locarnini et al.,* 2010]. Since the spin-up time is short, we used here the annual mean fields in order to mitigate the time-lag of deep layers of the solution during its annual cycle. Initial fields of velocity and ice concentration are zero. The calculations involved up to 1630 cores, storage costs were about 800 GB per model year. The data for analysis were stored as successive 5-day means. In (3), we used them to form the 90-day running means for the EMHT calculation.

3. Model Circulation Spin-Up

Since the experiment duration is rather short and the start from the state of rest requires some spin-up, first of all it is important to consider the degree of model circulation stabilization. The five-year period is obviously not enough for the full model ocean depth to gain the quasi-stable dynamical regime approximating the real ocean climate. However, it turns out that for studying the eddy heat transport we will need a smaller range of depths. It is shown in [*Gulev et al.,* 2003; *Marsh et al.,* 2009] that in the Atlantic north of 50°N most of the MHT is formed by the horizontal circulation in the upper ocean, but not by the meridional overturning circulation. In the Southern Ocean south of 35°S, according to [*Volkov et al.,* 2010], meridional overturning plays an important role, but its eddy component is negligible compared to the horizontal eddy heat transport. *Jayne and Marotzke* [2002] analyzed the results of numerical experiments in four depth intervals, and it was concluded that the zonal mean MHT at all latitudes is almost completely concentrated in the upper 1000-meter layer of the ocean. Observational data analysis in [*Qiu and Chen,* 2005] shows that specific correlations of temperature and velocity anomalies responsible for the formation of the eddy heat transport usually occur in the surface mixed layer.

Let us consider time-depth diagrams of the area-mean kinetic energy (per unit mass) at three representative locations of high eddy activity of different kinds to get a qualitative estimate of the degree of stabilization of the model velocity field (Figure 1): meandering of the Gulf Stream current after its separation from the shelf slope (31.5°–42.5°N, 56°–76°W), the Agulhas Retroflection region (35°–44°S, 10°–30°E), and the Eastern Equatorial Pacific demonstrating tropical instability waves (7.5°S–7.5°N, 115°–145°W).

It can be seen that local energetic characteristics of the solution in the regions of intense eddy activity become stable in the upper 1500-meter ocean layer during the first year of model integration. Thus we can conclude that, on a qualitative level, the experiment duration is enough for studying the global eddy heat transport. Meanwhile, the circulation stabilization in different regions occurs at a different rate, and sometimes it is accompanied by high interannual variability. Therefore, we chose the period for multi-year averaging of studied variables as the last four years of the experiment (1979–1982).

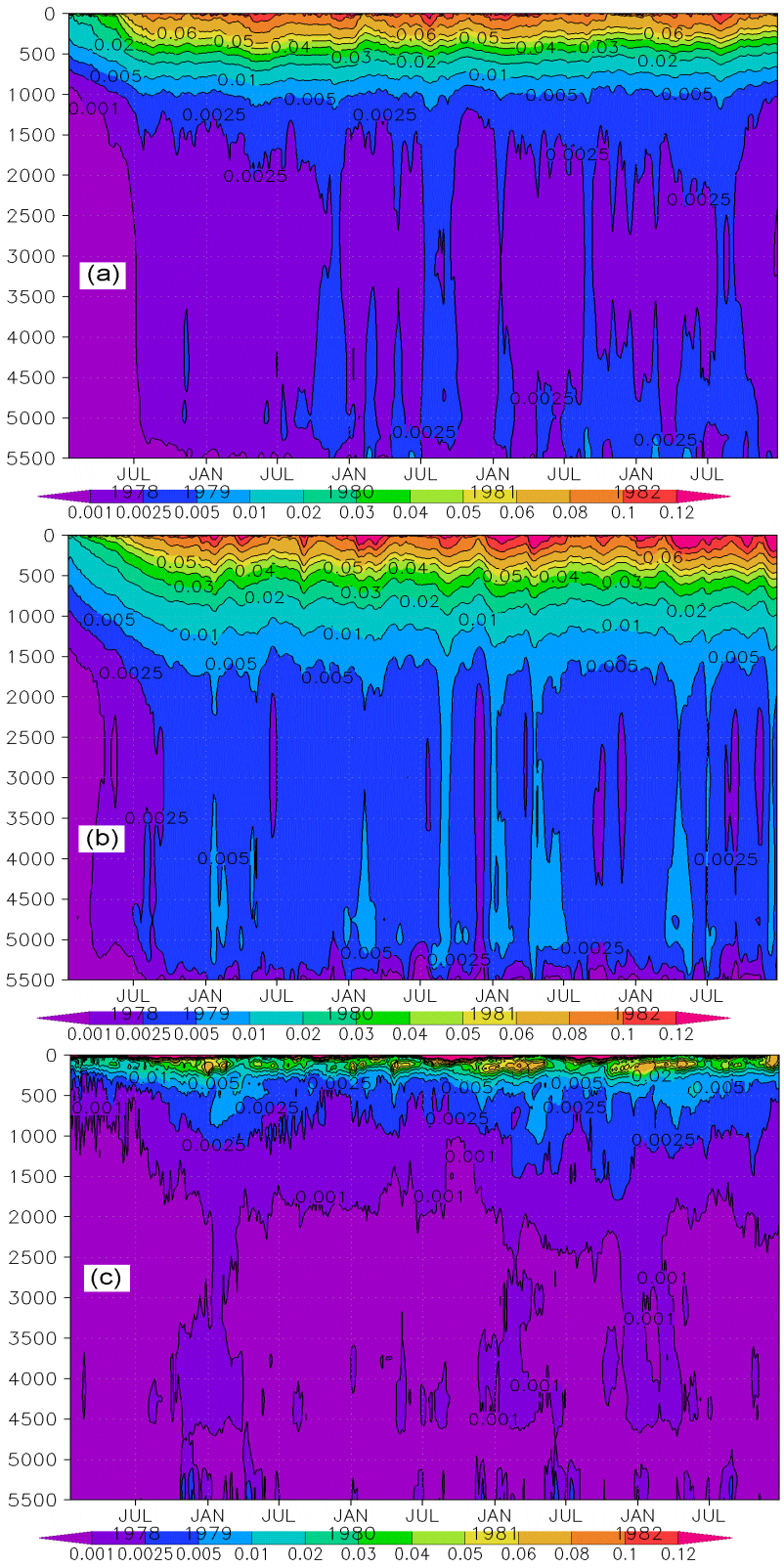

Figure 1. Time and depth distribution of area-mean kinetic energy per unit mass (m^2/s^2) in the regions of high eddy activity: Gulf Stream (31.5°–42.5°N, 56°– 76°W), Agulhas Retroflection (35°–44°S, 10°–30°E), and Eastern Equatorial Pacific (7.5°S–7.5°N, 115°–145°W).

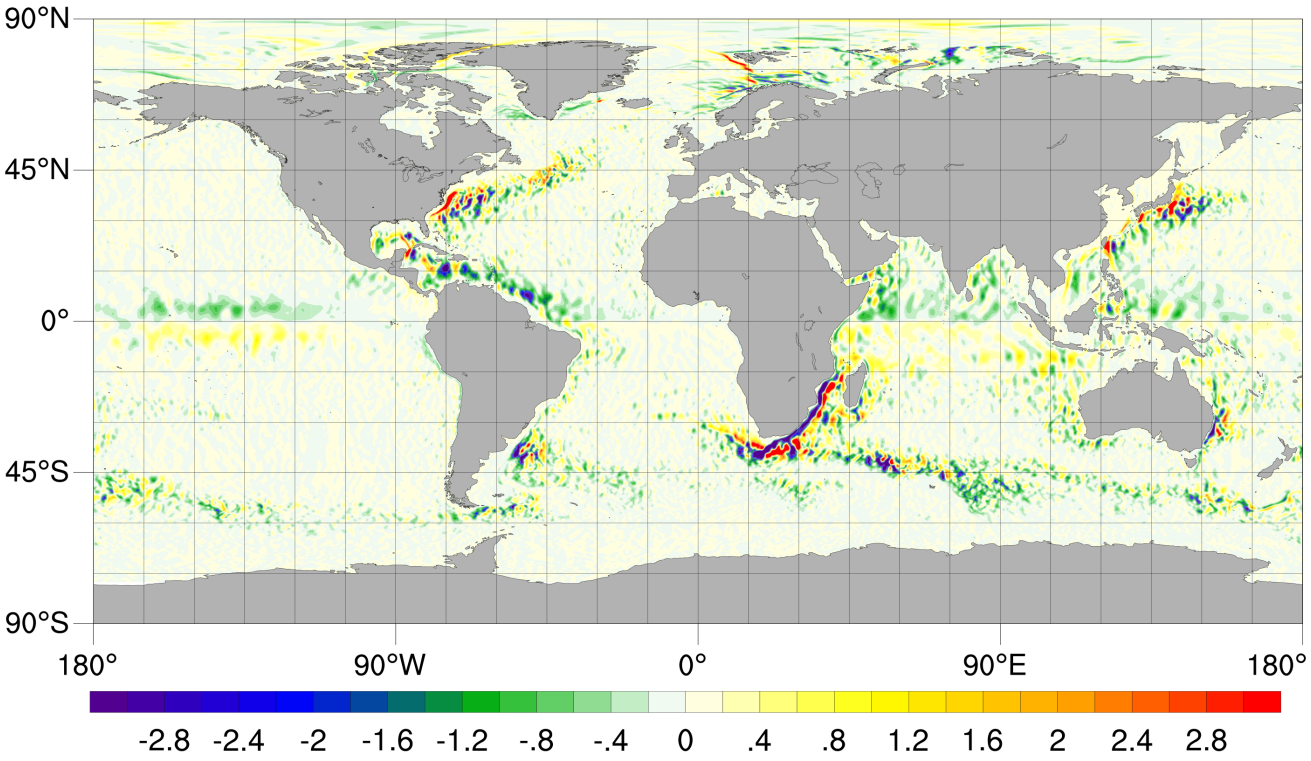

Figure 2. The EMHT integrated over full ocean depth, 10^8 W/m.

4. Results of the Model Experiment

4.1 Geographical Distribution of the EMHT

The geographical distribution of the eddy-active regions may be illustrated on the map of the EMHT integrated over depth from the ocean surface to bottom, which is shown in Figure 2 in the units of W per meter of the latitude circle.

As expected [*Wunsch,* 1999], we find high EMHT values in the regions of western boundary currents and current confluences, and also in the tropics, while in the ocean gyres the EMHT is small. The model Gulf Stream and Kuroshio are characterized by alternating zones of oppositely-directed EMHT which, in light of the multi-year averaging period, indicates the existence of stable pulsation structures, which make a significant regional contribution to the heat transport. Changing of the EMHT direction along the pathway of the currents supposes that the eddy heat transport sometimes occurs in the upgradient temperature direction (i.e., from cold to warm waters), which may lead to an overestimation of model integral EMHT values in case of their parameterization by a simple formula like (2) with a large positive coefficient A_H. Such a comparison is given by [*Jayne and Marotzke,* 2002; *Yim et al.,* 2010] for their modeling results and altimetry-based assessments by [*Stammer,* 1998; *Stammer et al.,* 2006]. Our Figure 3 illustrates this issue for the considered currents showing the EMHT and water temperature, integrated and averaged over the upper 100-meter layer, respectively. The effect of eddies manifests itself in the heat transported predominantly from the midstream to periphery, which conduces to deviation of isotherms from zonal direction south of the currents.

In the region of the Gulf Stream north of Cape Hatteras, the eddies also partially compensate the advection of cold by the coastal current from the north. Moreover, the magnitude of eddy heat flux here turns out to be one of the largest even on the global scale. Mean temperature and salinity fields obtained in this experiment were compared with the WOA09 data in [*Ushakov and Ibrayev,* 2017], and warm and salty bias of model data was found in the north near Cape Hatteras.

The model velocity field shows an anticyclonic meander attached to the shelf slope in this region.

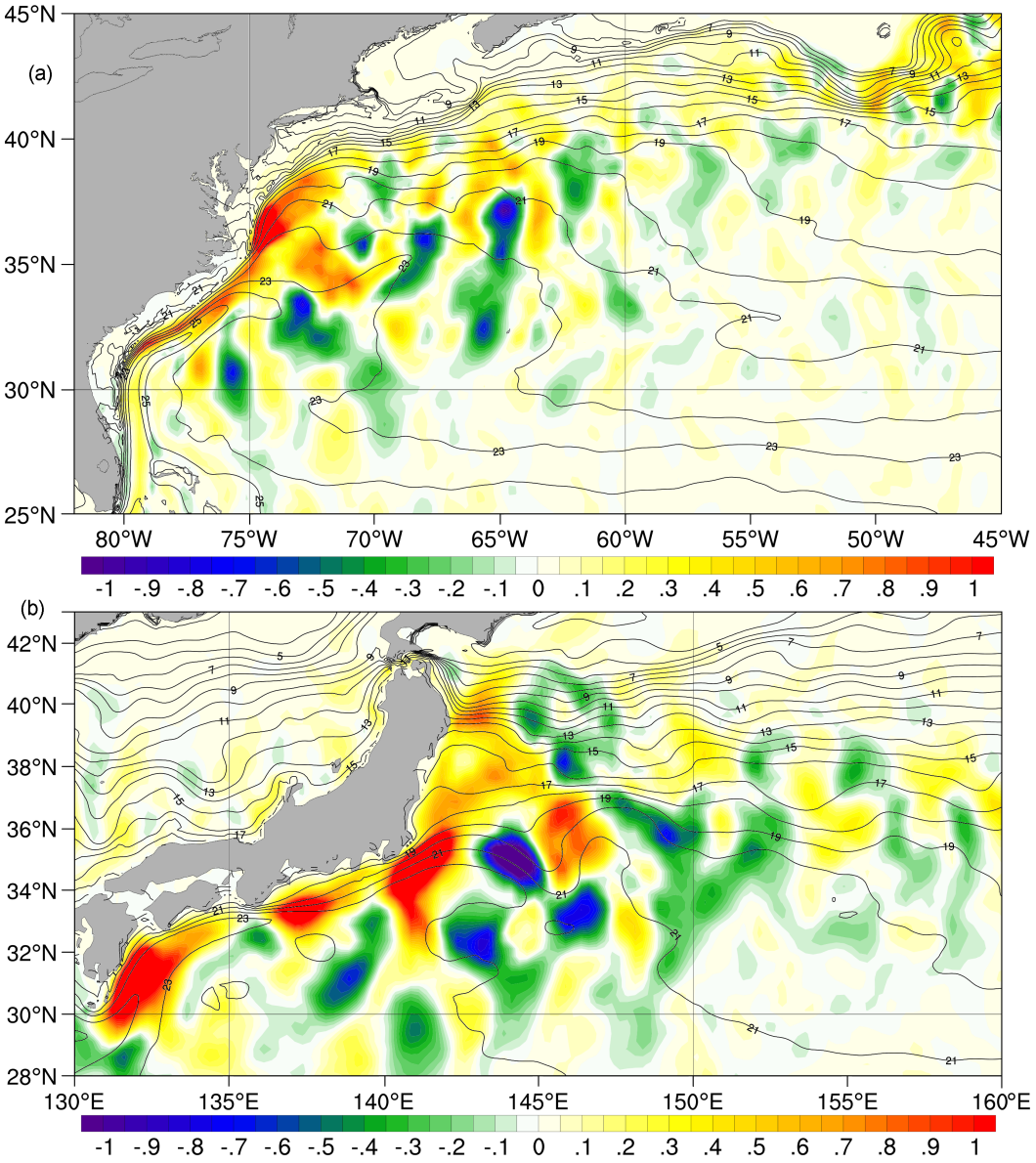

Figure 3. The EMHT in the Gulf Stream and Kuroshio regions integrated over the upper 100-meter ocean layer (color scale, 10^8 W/m), and temperature averaged over this depth interval (°C, isolines).

Besides, the model current can split into two branches: a warm tongue spreading into the open ocean, and a shelf branch that forms the temperature front. This phenomenon sometimes occurs in nature (see, for example, the NOAA data archive (Monaldo F. (1997), Primer on the Estimation of Sea Surface Temperature Using TeraScan Processing of NOAA A VHRR Satellite Data Version 2.0. The Johns Hopkins University, Applied Physics Laboratory. http://fermi.jhuapl.edu/avhrr/avhrr/gs/averages/07jun/gs_07jun22_2223_multi.png). But on the quantitative level this is a model bias, which does not agree with the mean observational data, e.g., [*Sarkisyan et al.,* 2016]. Traditionally, this bias is interpreted as the current deviation to the north, characteristic of the models with coarse resolution and/or large viscosity and diffusion coefficients [*Bryan et al.,* 2007; *Griffies et al.,* 2009]. It was assumed in [*Williams et al.,* 2012] that the correct reproduction of the Gulf Stream path is defined by sufficient level of eddy heat transport in the model solution. There is no explicit (Lapla-

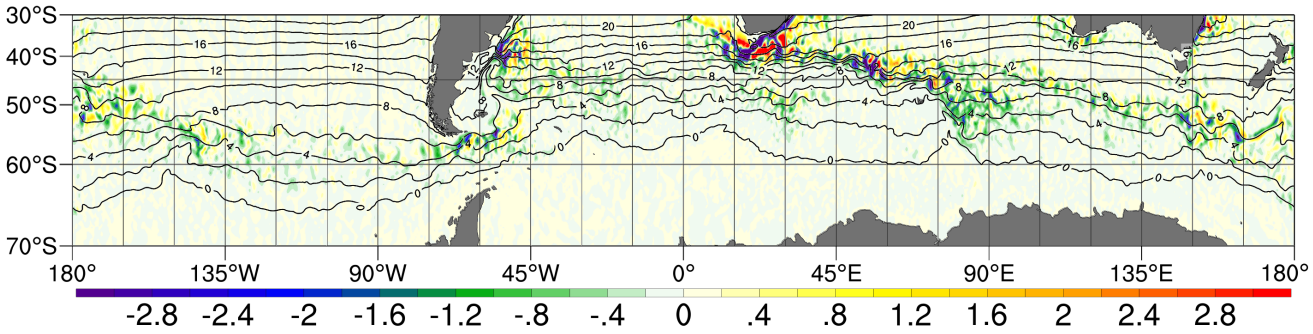

Figure 4. The EMHT integrated over the total ocean depth (color scale, 10^8 W/m) and sea surface temperature (isolines, °C).

cian) viscosity in our experiment; while analysis of diffusive heat fluxes (the third term in (3)) showed that they are negligible. However, the eddy heat northward transport from Cape Hatteras is large and contributes significantly to overheating of this region. This allows us to make an assumption that the mechanism of model Gulf Stream warm waters deviation from the observed path, which is still a challenge to many modern models, is related to the overestimation of the eddy activity, regardless of whether it is parameterized by the formula (2) or explicitly resolved. The possible cause of the bias in our case may be a still excessive value of the diffusion coefficient. At the same time, there is no such problem for Kuroshio in our results, and the current separation location is reproduced qualitatively right.

In the Southern Ocean, the major part of the MHT is provided by the stationary global scale meandering of the ACC, which carries warm waters to the southeast from Africa in the Indian Ocean and cold waters to the north from the Drake Passage in the Atlantic [*Volkov et al.,* 2010]. According to our calculations, the EMHT is significant at the northern edge of the ACC; it approximately follows the surface isotherms in the Polar Front Zone (Figure 4). It reaches the maximal values in the regions of the Agulhas Retroflection (on the Subtropical Front) and in the Zapiola Anticyclone and Brazil-Malvinas Confluence Zone.

The role of the EMHT is also important in the Drake Passage, where the meridional transport of mean almost zonal current is generally small. The model reproduces high eddy activity south of Tasmania and of New Zealand, and several ACC jets modulated by the bottom topography. Their number is maximal in the Atlantic and Indian sectors of the Southern Ocean, which agrees with observational and other model data (see, e.g., [*Volkov et al.,* 2010] and references therein).

The characteristic feature of the Agulhas Current is a strong EMHT "jet", which approximately coincides with the mean flow jet in position and direction, and is formed apparently by the current meandering. At the southern periphery of the jet, the EMHT is oppositely directed, which may be caused by formation of rings. The EMHT structure of the former (jet) kind turned out to be characteristic of the East Australian Current, and the structure of the latter one (peripheral) is characteristic of the North Brazil Current. The model also reproduces the northwestward transport of the Agulhas rings in the South Atlantic, which is an important factor of exchange between the Indian and Atlantic oceans.

Finally, a significant contribution to the total tropical MHT is made by the equatorward eddy heat transport due to the tropical instability waves, mainly in the Pacific Ocean. Here, eddies warm the well-known cold tongue of East-Pacific waters. Figure 5 presents the meridional distribution of the equatorial EMHT convergence according to our experiment (integrated over the full ocean depth in the band from 0.125°S to 0.125°N) compared to the other model data [*Jayne and Marotzke,* 2002] and to the assessment in [*Bryden and Brady,* 1989] based on the moored current meter data in 1979–1981.

Obviously, the zonal means of the model EMHT convergence in the 110°W–140°W band are nearly equal based on the INMIO (177 W/m^2) and [*Jayne and Marotzke,* 2002] (190 W/m^2). The mean INMIO value for the 110°W–152°W interval (158 W/m^2) appeared close to the lower limit

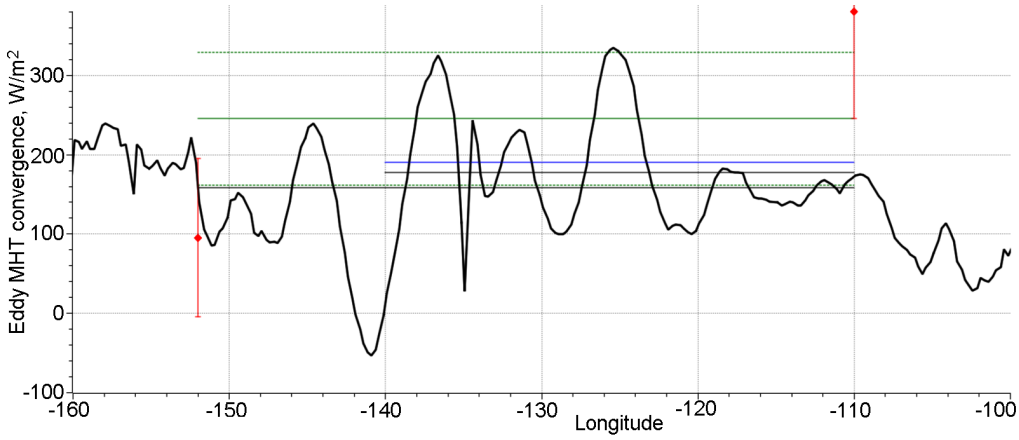

Figure 5. Meridional distribution of the EMHT convergence at the equator (W/m^2). The black thick curve presents the INMIO model data. The solid blue and green lines are zonal mean values from [*Jayne and Marotzke,* 2002] and [*Bryden and Brady,* 1989], thin black lines denote the zonal mean INMIO values in respective longitude ranges. Dashed green lines show the error estimate of the zonal mean value in [*Bryden and Brady,* 1989]. Red diamonds with error bars are data from [*Bryden and Brady,* 1989] at 110°W and 152°W.

of estimated error of the analogous mean in [*Bryden and Brady,* 1989] (245 ± 84 W/m^2). To a notable extent, this is due to the eddy heat transport fluxes divergence from the equator at 141°W (-54 W/m^2), where these fluxes have upgradient components relative to the temperature horizontal levels (Figure 6).

The error estimation interval in [*Bryden and Brady,* 1989] at 152°W (95 ± 100 W/m^2) covers the INMIO result (164 W/m^2). However, at 110°W the INMIO model EMHT convergence appeared much less than that in [*Bryden and Brady,* 1989] (380 ± 135 W/m^2). At the latter location, the model in [*Jayne and Marotzke,* 2002] showed a convergence qualitatively similar to our result (considering their mean value equal to 190 W/m^2 and the distribution in their Figure 8a). The drifter-based estimate [*Hansen and Paul,* 1984] suggests a higher value, since they obtain 180 W/m^2 only in the upper 50-meter layer in the 105°W–120°W band. Hence, we can assume that such a difference between the modeled and observed data in the far Eastern Pacific is systematic. Its causes are to be established in future studies.

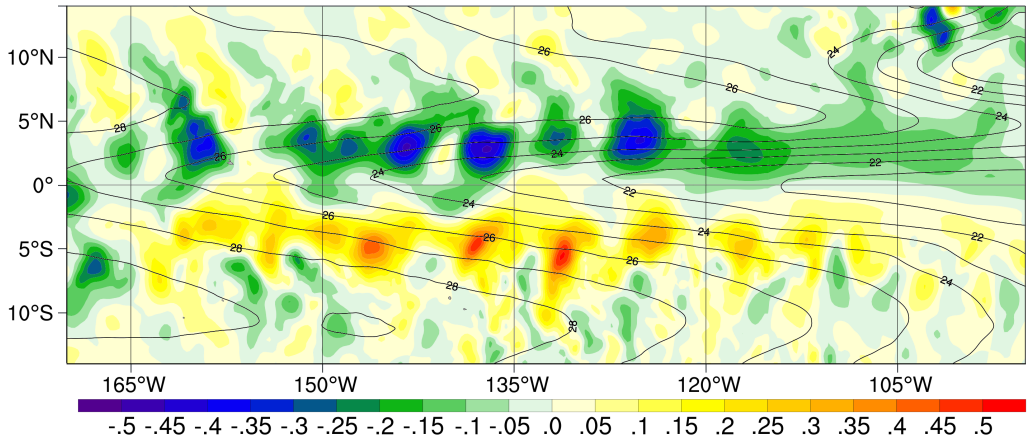

Figure 6. The Eastern Pacific equatorial EMHT integrated over the upper 100-meter ocean layer (color scale, 10^8 W/m), and temperature averaged over this depth interval (°C, isolines).

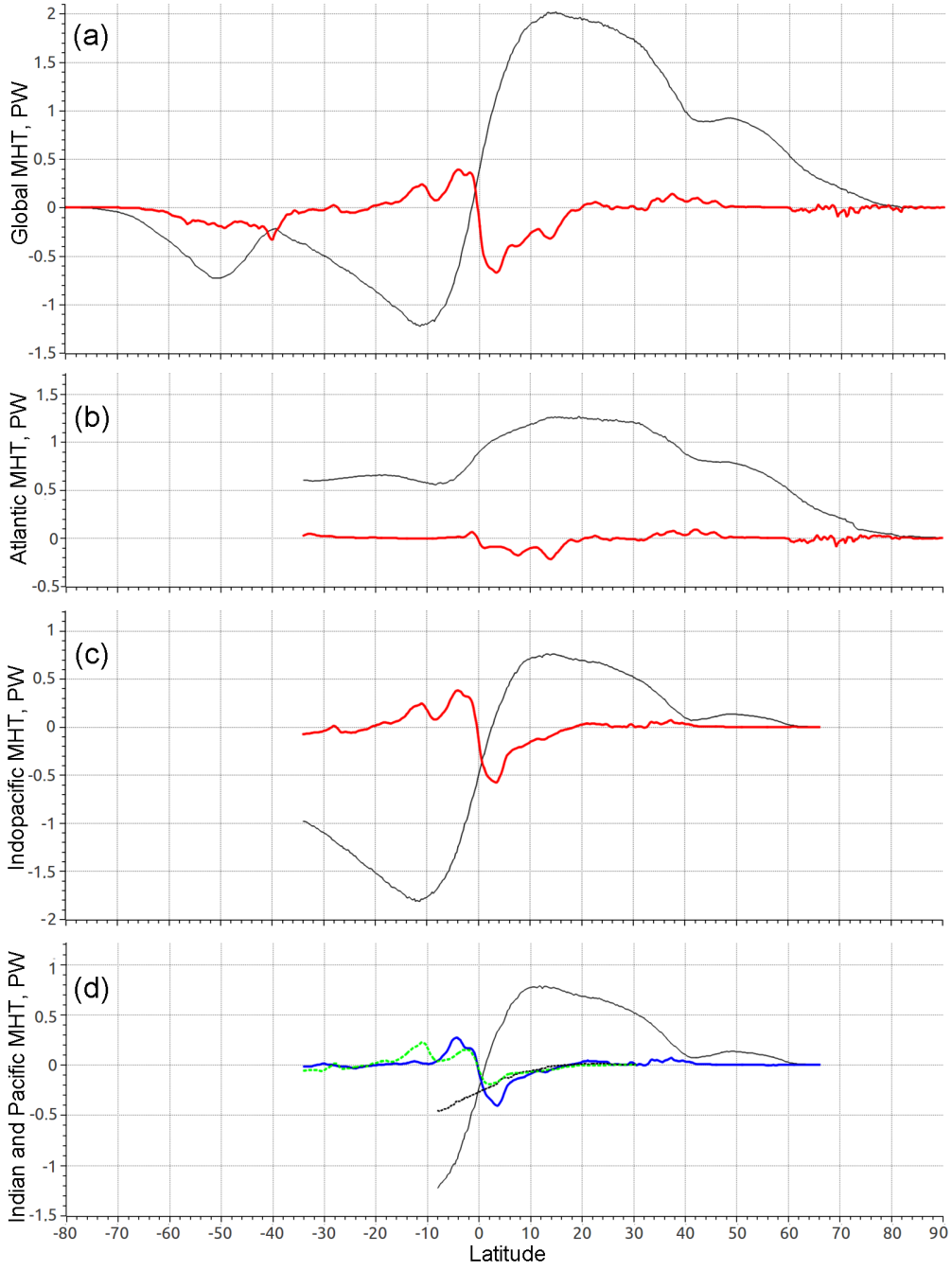

Figure 7. Distributions of the zonally integrated total (thin black lines) and eddy-induced (thick color lines) MHT in: (a) the world ocean, (b) the Atlantic Ocean, (c) the Indo-Pacific basin, and (d) the Indian and Pacific oceans separately (dashed and solid lines, respectively).

4.2. Integral EMHT Distribution

On the global scale, the distribution of the model EMHT, integrated over depth and zonal direction, is shown in Figure 7 for the world ocean and its large basins. The total MHT is also given for comparison. Negative (positive) slope of the graph indicates integral heating (cooling) of the ocean by advective heat transport at the given latitude. It can be seen that at many latitudes the eddy component makes a significant contribution to the total MHT.

Usually, when studying the integral MHT in the world ocean basins, the Indian and Pacific oceans are treated together as a single basin due to a substantial water exchange between them by the Indonesian Throughflow. However, since the flow through the Malacca Strait (as well as through the Bering Strait) is small, we assume that it is possible to take zonal sections with zero total water transport in the Indian and Pacific oceans separately at all latitudes north of Java Island (8°S). Hence, at these latitudes it is possible to consider the MHTs of the Indian and Pacific oceans separately. As for the EMHT, since it is determined by the anomalies of temperature and velocity, its long-term means make sense for all latitudes of both oceans. At the same time, they may include a component caused by the intra-seasonal variability of the Indonesian Throughflow.

Graphs for all oceans show that the EMHT is small at 20°–35°S latitudes, and hence the southward EMHT of the western boundary currents is almost compensated by the opposite eddy transport of the open ocean. This disagrees with the study in [*Meijers et al.,* 2007] (and, to some extent, in [*Volkov et al.,* 2008]) where the near-shore eddy transport prevails over a part of this latitudinal band. The South Atlantic EMHT at 30°–33°S is positive (up to 0.05 PW) due to the Agulhas rings. At 40°S, which is the latitude of the Agulhas Retroflection and the Brazil-Malvinas Confluence, the eddy component of the MHT is most significant. It exceeds the MHT of the mean flow and reaches −0.33 PW which is approximately equal to the results of [*Jayne and Marotzke,* 2002; *Meijers et al.,* 2007; *Volkov et al.,* 2008], but slightly smaller in magnitude than those of [*Griffies et al.,* 2015; *Volkov et al.,* 2010].

South of 40°S, the mean MHT changes sign, and soon its magnitude exceeds that of the EMHT, which in turn decreases and becomes negligible approximately at 60°S, which is the southern edge of the ACC. A similar zonal distribution was obtained by high-resolution models [*Griffies et al.,* 2015; *Meijers et al.,* 2007], while more coarse configurations [*Jayne and Marotzke,* 2002; *Volkov et al.,* 2008, 2010] as well as the low-resolution version of [*Griffies et al.,* 2015] extend the zone of notable EMHT farther to the south.

In the Southern Ocean, our model EMHT magnitude is generally less than that given in the above mentioned works. This may be caused because we used a rather narrow timescale filter with a window of only 90 days in formula (3), which in the case of the Southern Ocean may lead to an underestimation of effect of specific eddy structures that are mesoscale in space but have longer time scales [*Volkov et al.,* 2010]. This assumption is supported by the fact that both [*Volkov et al.,* 2008] and [*Volkov et al.,* 2010] used the same model data of the ECCO2 project, but with different filter windows (3 months and 10 years); they obtained substantially different magnitudes of the EMHT at 30°S (−0.3 and −0.5 PW, respectively).

Equatorial regions receive a substantial contribution of eddy heat transport, related to the tropical instability waves and partially compensating the divergent Ekman poleward transport. The near-equator extrema of the integral EMHT in the world ocean are located at 1.7°S and 3.4°N constituting 0.36 PW and −0.67 PW, respectively. The southern integral extremum is nearly equally distributed between the Indian and Pacific oceans, with a small contribution of the Atlantic (about 0.05 PW). The northern one is mainly determined by the Pacific Ocean (−0.41 PW). Similar results were obtained in [*Volkov et al.,* 2008] with a coarser resolution, but in our case the EMHT extrema are higher and located closer to the equator. The absolute maximum of the northward EMHT is located at 3.9°S. It is formed mainly by the tropical instability waves of the Pacific Ocean, where their local EMHT reaches the maximal values (Figure 6).

At greater distances from the equator there are secondary peaks of the global integrated EMHT: 0.24 PW at 11°S and −0.32 PW at 13.7°N. The former is formed almost exclusively at the northern edge of the South Equatorial Current in the Indian Ocean. The latter by about two thirds is formed in the Atlantic by the North Brazil and Caribbean currents, and also by the tropical instability waves. This is a qualitative difference between our experiment and the study in [*Volkov et al.,* 2008], where the Pacific EMHT dominates at these latitudes of the Northern Hemisphere.

Farther to the north, at the latitudes of Atlantic and Pacific western boundary currents, mesoscale eddies carry heat northward. The eddy activity of the Kuroshio and the North Pacific Current is notable in the 32°–42°N interval with the maximum equal to 0.07 PW. The EMHT constitutes

a significant part of the total MHT in the northern part of this latitude band. Significant EMHT values of the Gulf Stream and the North Atlantic Current spread northward up to 48°N and reach 0.09 PW. Both these local EMHT extrema are 2–3 times lower than those given in [*Griffies et al.,* 2015] obtained with the same spatial resolution. Besides the different filter windows, this decrease could be related to a less-zonal path of the Gulf Stream, as suggested by [*Griffies et al.,* 2015].

The eddy heat transport of the Arctic Ocean, particularly of its Atlantic sector, deserves an individual study. Our experiment revealed relatively high (from −0.08 to 0.03 PW) values of the zonally integrated EMHT in this sector over the pathway of the North Atlantic Current branches.

5. Conclusion

This work follows the line of oceanology, which studies mesoscale eddies and their impact on the world ocean heat budget by means of numerical modeling. It is aimed at continuing the series of researches of many authors [*Griffies et al.,* 2015; *Jayne and Marotzke,* 2002; *Volkov et al.,* 2008, 2010; *Yim et al.,* 2010, and others], in which growing computational resources are utilized to study the eddy-induced meridional heat transport with increasing resolution and geographic scope. We performed a five-year numerical experiment on the simulation of the world ocean EMHT by the INMIO model with 0.1° resolution under the CORE-II conditions. The eddy-induced MHT component was defined as the deviation of the total MHT from the one based on the mean temperature and velocity fields. We assessed global magnitudes and distribution of the EMHT. The results of our experiment generally agree with the above mentioned studies and justify the trend for growing of the absolute values of the EMHT and its concentrating in specific locations as the model resolution increases. The eddy heat transport appears to be significant in many regions of the world ocean, and it is not always possible to perform unambiguous parameterization by the traditional heat diffusion formula. This is mainly related to the locations where the EMHT has an upgradient component relative to the horizontal temperature field. Thus, it seems reasonable to use at least eddy-permitting models when studying the world ocean heat budget.

The specific feature of this study is a rather small window (90 days) of the running mean procedure used for extraction of the MHT eddy component, while most other studies (except [*Volkov et al.,* 2008]) make their means over a year or over the total experiment duration. Considering the large volume of the processed data, our technique is more expensive, but in general it seems more reasonable, since it does not mix the effects of mesoscale eddies with the effects of longer term variability. Possibly due to this fact, we obtained lower values of the EMHT in some regions. Hence, the model verification and correct comparison requires that in the other studies it is necessary to assess the sensitivity of the obtained eddy heat transport to characteristics of the filter, especially in regions where long-living mesoscale eddies are observed.

Besides that, we obtained some qualitative differences with the results of other modeling and observational studies. Particularly, they are related to the values of the EMHT convergence in the Equatorial East Pacific and the ratio of the EMHTs of the Atlantic and Pacific North Tropical zones. A detailed analysis of these issues presents a good topic for further studies.

Acknowledgments. The authors dedicate this work to the memory of Academician Artem S. Sarkisyan, who was one of the initiators of the numerical ocean modeling in the USSR and made a great contribution to this field of science and to the INMIO model development. The computations were carried out on MVS-10P at Joint Supercomputer Center of the Russian Academy of Sciences (JSCC RAS). This research was performed in the framework of the state assignment of FASO Russia (Presidium of RAS program No. 49 “Interaction of physical, chemical and biological processes in the world ocean”), supported in part by RFBR (project No. 16-05-01101).

References

Antonov, J. I., D. Seidov, T. P. Boyer, et al. (2010), *World ocean Atlas 2009, Volume 2, Salinity. S. Levitus (Ed.), NOAA Atlas NESDIS 69*, U.S. Government Printing Office, Washington, D.C.

Beckmann, A., J. Willebrand, et al. (1994), Effects of increased horizontal resolution in a simulation of the North Atlantic Ocean, *J. Phys. Oceanogr., 24,* 326–344,**Crossref**

Bryan, F. O., M. W. Hecht, R. D. Smith (2007), Resolution convergence and sensitivity studies with North Atlantic circulation models. Part I: The western boundary current system, *Ocean Modelling*, *16,* 141–159,Crossref

Bryan, K. (1969), A numerical method for the study of the circulation of the world ocean, *J. Comp. Phys.*, *4,* No. 3, 347–376,Crossref

Bryan, K. (1996), The role of mesoscale eddies in the poleward transport of heat by the oceans: A review, *Physica D*, *98,* 249–257,Crossref

Bryden, H. L., E. C. Brady (1989), Eddy momentum and heat fluxes and their effects on the circulation of the equatorial Pacific Ocean, *J. Mar. Res.*, *47,* 55–79,Crossref

Diansky, N. A., E. M. Volodin (2002), Simulation of present-day climate with a coupled atmosphere-ocean general circulation model, *Izvestiya, Atmospheric and Oceanic Physics*, *38,* No. 6, 732–747.

Diansky, N. A., A. V. Bagno, V. B. Zalesny (2002), Sigma model of global ocean circulation and its sensitivity to variations in wind stress, *Izvestiya, Atmospheric and Oceanic Physics*, *38,* No. 4, 477–494.

Dong, C., J. C. McWilliams, Yu Liu, D. Chen (2014), Global heat and salt transports by eddy movement, *Nat. Commun.*, *5,* 3294,Crossref

Flierl, G., J. C. Mcwilliams (1977), Sampling requirements for measuring moments of eddy variability, *J. Mar. Res.*, *35,* 797–820.

Ganachaud, A., C. Wunsch (2003), Large-scale ocean heat and freshwater transports during theworld ocean Circulation Experiment, *J. Clim.*, *16,* 696–705,Crossref

Gill, A. E. (1982), *Atmosphere–Ocean Dynamics*, 662 pp., Academic Press, Moscow.

Griffies, S. M. (2006), Some Ocean Model Fundamentals, *Ocean Weather Forecasting, Chassignet E. P., Verron J. (eds.)* p. 19–73, Springer, Dordrecht.Crossref

Griffies, S. M., et al. (2009), Coordinated ocean-ice reference experiments (COREs), *Ocean Modelling*, *26,* No. 1–2, 1–46,Crossref

Griffies, S. M., et al. (2012), *Datasets and protocol for the CLIVAR WGOMD Coordinated Ocean-sea ice Reference Experiments (COREs). WCRP Report No. 21/2012*, 23 pp., International CLIVAR Project Office, Southampton.

Griffies, S. M., et al. (2015), Impacts on Ocean Heat from Transient Mesoscale Eddies in a Hierarchy of Climate Models, *J. Climate*, *28,* 952–977,Crossref

Gulev, S., B. Barnier, H. Knochel, J. Molines, M. Cottet (2003), Water mass transformation in the North Atlantic and its impact on the meridional circulation: insights from an ocean model forced by NCEP-NCAR reanalysis surface fluxes, *J. Clim.*, *16,* No. 19, 3085–3110,Crossref

Gusev, A. V., N. A. Diansky (2014), Numerical simulation of the world ocean circulation and its climatic variability for 1948–2007 using the INMOM, *Izvestiya, Atmospheric and Oceanic Physics*, *50,* No. 1, 1–12,Crossref

Hall, M. M., H. L. Bryden (1982), Direct estimates and mechanisms of ocean heat transport, *Deep Sea Research Part A. Oceanographic Research Papers*, *29,* No. 3, 339–359,Crossref

Hansen, D. V., C. A. Paul (1984), Genesis and effects of long waves in the equatorial Pacific, *J. Geophys. Res.*, *89,* 10,431–10,440,Crossref

Ibrayev, R. A. (2001), Model of enclosed and semi-enclosed sea hydrodynamics, *Russ. J. Numer. Anal. Math. Modelling*, *16,* No. 4, 291–304,Crossref

Ibrayev, R. A., R. N. Khabeev, K. V. Ushakov (2012), Eddy-resolving 1/10° model of the world ocean, *Izvestiya, Atmospheric and Oceanic Physics*, *48,* No. 1, 37–46,Crossref

Jayne, S. R., J. Marotzke (2002), The oceanic eddy heat transport, *J. Phys. Oceanogr.*, *32,* 3328–3345,Crossref

Kalmykov, V. V., R. A. Ibrayev (2013), The overlapping algorithm for solving shallow water equations on massively-parallel architectures with distributed memory, *Vestnik UGATU*, *17,* No. 5 (58), 252–259. (in Russian)

Kalmykov, V. V., R. A. Ibrayev, K. V. Ushakov (2014), Problems and challenges in creating a high-resolution Earth system model, *Supercomputer Technologies in Science, Education and Industry* p. 14–22, MSU Publishers, Moscow. (in Russian)

Lebedev, V. I. (1964a), Difference analogues of orthogonal decompositions, basic differential operators and some boundary problems of mathematical physics. I, *USSR Computational Mathematics and Mathematical Physics*, *4,* No. 3, 69–92,Crossref

Lebedev, V. I. (1964b), Difference analogues of orthogonal decompositions, basic differential operators and some boundary problems of mathematical physics. II, *USSR Computational Mathematics and Mathematical Physics*, *4,* No. 4, 36–50,Crossref

Locarnini, R. A., A. V. Mishonov, J. I. Antonov, T. P. Boyer, H. E. Garcia, O. K. Baranova, M. M. Zweng, D. R. Johnson (2010), *World ocean Atlas 2009, Volume 1: Temperature. S. Levitus (Ed.), NOAA Atlas NESDIS 68*, 184 pp., U.S. Government Printing Office, Washington, D.C.

Macdonald, A. M., C. Wunsch (1996), An estimate of global ocean circulation and heat fluxes, *Nature*, *382,* 436–439,Crossref

Maltrud, M. E., J. L. McClean (2005), An eddy resolving global 1/10° ocean simulation, *Ocean Model.*, *8,* 31–54,Crossref

Marsh, R., B. A. de Cuevas, A. C. Coward, et al. (2009), Recent changes in the North Atlantic circulation simulated with eddy-permitting and eddy-resolving ocean models, *Ocean Model.*, *28,* No. 4, 226–239,Crossref

Marzocchi, A., et al. (2015), The North Atlantic subpolar circulation in an eddy-resolving global ocean model, *J. Marine Sys.*, *142,* 126–143,Crossref

Meijers, A. J., N. L. Bindoff, J. L. Roberts (2007),

On the Total, Mean, and Eddy Heat and Freshwater Transports in the Southern Hemisphere of a $1/s^\circ \times 1/s^\circ$ Global Ocean Model, *J. Phys. Oceanogr.*, *37,* 277–295,Crossref

Mesinger, F., A. Arakawa (1976), *Numerical Methods Used in Atmospheric Models, GARP Publ. Series # 17, V. I*, 64 pp., WMO/ISCU Joint Org. Committee, Geneva.

Morrison, A. K., O. A. Saenko, A. M. Hogg, et al. (2013), The role of vertical eddy flux in southern ocean heat uptake, *Geophys. Res. Lett.*, *40,* 5445–5450,Crossref

Munk, W. H., E. R. Anderson (1948), Note on the theory of the thermocline, *J. Mar. Res.*, *7,* 276–295.

Murray, R. J. (1996), Explicit generation of orthogonal grids for ocean models, *J. Comp. Phys.*, *126,* No. 2, 251–273,Crossref

Polonsky, A. B., S. B. Krasheninnikova (2015), Variability of the Currents' Vertical Structure in the Western Subtropical Atlantic and Meridian Heat Transport, *Physical Oceanography*, *3,* 35–49,Crossref

Qiu, B., S. Chen (2005), Eddy-induced heat transport in the subtropical North Pacific from Argo, TMI, and altimetry measurements, *J. Phys. Oceanogr.*, *35,* 458–473,Crossref

Roemmich, D., J. Gilson (2001), Eddy transport of heat and thermocline waters in the North Pacific: A key to interannual/decadal climate variability?, *J. Phys. Oceanogr.*, *31,* 675–687,Crossref

Sarkisyan, A. S., J. E. Sündermann (2009), *Modelling Ocean Climate Variability*, 374 pp., Springer, Dordrecht, Netherlands.Crossref

Sarkisyan, A. S., O. P. Nikitin, K. V. Lebedev (2016), Physical characteristics of the Gulf Stream as an indicator of the quality of large-scale circulation modeling, *Doklady Earth Sciences*, *471,* No. 2, 1288–1291,Crossref

Schrum, C., J. Backhaus (1999), Sensitivity of atmosphere-ocean heat exchange and heat content in North Sea and Baltic Sea. A comparative Assessment, *Tellus*, *51A,* 526–549,Crossref

Smith, R. D., et al. (2000), Numerical simulation of the North Atlantic Ocean at 1/10°, *J. Phys. Oceanogr.*, *30,* 1532–1561,Crossref

Stammer, D. (1998), On eddy characteristics, eddy transports, and mean flow properties, *J. Phys. Oceanogr.*, *28,* 727–739,Crossref

Stammer, D., C. Wunsch, K. Ueyoshi (2006), Temporal changes in ocean eddy transports, *J. Phys. Oceanogr.*, *36,* 543–550,Crossref

Ushakov, K.V., R.A. Ibrayev, V.V. Kalmykov (2015), Simulation of the world ocean climate with a massively parallel numerical model, *Izvestiya, Atmospheric and Oceanic Physics*, *51,* No. 4, 362–380,Crossref

Ushakov, K. V., T. B. Grankina, R. A. Ibrayev (2016), Modeling the water circulation in the North Atlantic in the scope of the CORE-II experiment, *Izvestiya, Atmospheric and Oceanic Physics*, *52,* No. 4, 365–375,Crossref

Ushakov, K. V., R. A. Ibrayev (2017), Simulation of the global ocean thermohaline circulation with an eddy-resolving INMIO model configuration, *IOP Conf. Ser.: Earth Environ. Sci.*, *96,* 012007,Crossref

Volkov, D. L., T. Lee, L.-L. Fu (2008), Eddy-induced meridional heat transport in the ocean, *Geophys. Res. Lett.*, *35,* L20601,Crossref

Volkov, D. L., L.-L. Fu, T. Lee (2010), Mechanisms of the meridional heat transport in the Southern Ocean, *Ocean Dynamics*, *60,* 791–801,Crossref

Volodin, E. M., et al. (2018), Reproduction of world ocean circulation by the CORE-II scenario with the models INMOM and INMIO, *Izvestiya, Atmospheric and Oceanic Physics*, *54,* No. 1, 86–100,Crossref

Williams, S., M. Petersen, M. Hecht, M. Maltrud, et al. (2012), Interface Exchange as an Indicator for Eddy Heat Transport, *Computer Graphics Forum*, *31,* 1125–1134,Crossref

Wunsch, C. (1999), Where do ocean eddy heat fluxes matter?, *J. Geophys. Res.*, *104,* 13,235–13,249,Crossref

Yim, B. Y., Y. Noh, B. Qiu, S. H. You, J. H. Yoon (2010), The vertical structure of eddy heat transport simulated by an eddy-resolving OGCM, *J. Phys. Oceanogr.*, *40,* 340–353,Crossref

Zalezak, S. T. (1979), Fully multidimensional flux-corrected transport algorithm for fluids, *J. Comput. Phys.*, *31,* 335–362,Crossref

R. A. Ibrayev, Shirshov Institute of Oceanology, Russian Academy of Sciences, 36 Nahimovskiy prospekt, 117997 Moscow, Russia.

K. V. Ushakov, Institute of Numerical Mathematics, Russian Academy of Sciences, 8 Gubkina str., 119333 Moscow, Russia. (ushakovkv@mail.ru)